Acta Biochimica Polonica

Vol. 44 No. 4/1997

627–644

QUARTERLY

This paper is dedicated to Professor Włodzimierz Ostrowski
Review

Intramolecular electron transfer between tryptophan radical and tyrosine in oligoproline-bridged model peptides and hen egg-white lysozyme

Kazimierz L. Wierzchowski✉

Institute of Biochemistry and Biophysics, Polish Academy of Sciences, A. Pawińskiego 5a, 02-106 Warsaw, Poland

Key words: intramolecular electron transfer, electron transfer pathways, pulse radiolysis, tryptophan radical, tyrosine radical, radical transformation, oligoproline peptides, hen egg-white lysozyme

Long range electron transfer (LRET) across protein matrix underlies all one-electron cellular redox reactions. Elucidation of molecular electron transfer pathways and parametrization of their relative efficiency is one of the most chalenging problems in the studies on LRET in proteins. In this paper results of pulse radiolysis investigations on kinetics of LRET accompanying intramolecular radical transformation $Trp^{\bullet} \rightarrow TyrO^{\bullet}$ in model peptides built of tryptophan and tyrosine bridged by an oligoproline fragment are reviewed, along with an interpretation of the observed distance dependence of the rate of LRET in terms of conformational properties of the peptides, and partitioning of LRET between electron transfer pathways through space and through peptide backbone. This review on model peptide systems is supplemented with recapitulation of similar studies on the same intramolecular transformation in hen egg-white lysozyme, which allowed to identify $Trp^{\bullet}$/Tyr redox pairs and associated electron transfer pathways involved in LRET in this protein.

It is now commonly accepted that long range electron transfer (LRET) between various donor-acceptor pairs located at a distance up to 3 nm within single redox proteins or between their functional complexes is a fundamental process underlying biological redox reactions. This is evidenced for the most part by the results of numerous experimental studies on electron transfer in selected protein systems [1, 2] involved in conversion of light into chemical energy in photosynthetic reaction centers, reduction of dioxygen to water in the mitochondrial respiratory chain, and in model ruthenium-modified metalloproteins like cytochrome *c* and myoglobin. Current understanding of the LRET mechanism relies on the theory of nonadiabatic one-electron transfer in chemical reactions, developed by R. Marcus [3, 4] in conjunction with various theoretical quantum-mechani-

✉Phone: 658-47-29; fax: (0-22) 658-46-36; e-mail: klw@ibbrain.ibb.waw.pl

Abbreviations: A, acceptor; D, donor; ET, electron transfer; HEWL, hen egg-white lysozyme; LRET, long range electron transfer; NFKyn, *N*-formylkynurenine; PLP II, polyproline II; TB and TS, electron transfer through peptide backbone and through space, respectively.

cal models of electron tunneling between the donor and acceptor cofactors through protein matrix [1, 3, 5–8].

According to analytical formulation of the semiclassical theory [4]:

$$k_{ET} = (4\pi^3/h^2\,\lambda k_B T)\, H_{DA}^2 \exp\{-(\Delta G^0 + \lambda)^2/4\lambda k_B T\} \quad (1),$$

(where h and k_B are the Planck and Boltzman constants, respectively, and T is temperature in K), the electron transfer reaction rate, k_{ET}, from a donor (D) to an acceptor (A), at a fixed distance and orientation, is under control of: (i) nuclear interactions, partitioned into the reaction free energy ($-\Delta G^0$) and reorganization energy, λ, necessary for the D/A pair with its immediate molecular environment to attain the transition-state configuration for electron transfer (ET), and (ii) electronic coupling between D and A, the strength of which, H_{DA}^2, is predicted to decay exponentially with their separation distance.

Results of experimental studies on kinetics of LRET in various model systems [1–4], and in Ru(III)-derivatized metalloproteins [1, 7] provide convincing support to these predictions. The latter also indicate that β sheets seem to mediate coupling more efficiently than α-helical structures. However, much more experimental and theoretical work is still needed for a more detailed description at the atomic level of how the effciency of LRET is controlled by various structural protein motifs.

In view of the complex structure of protein matrix separating DA centers, in parallel with the studies on redox proteins, various oligopeptide bridged DA systems were also studied as models of protein ET pathways. Earlier studies on unpaired electron transfer involving natural aromatic (Trp,Tyr) and aromatic and sulphur centers in flexible glycine bridged systems [9–14] showed that this process occurs for the most part through direct contacts between members of D/A pairs. Regarding the distance dependence of LRET most successful so far proved to be the systems built of oligoproline bridges, apt to attain in aqueous solution at polymerization numbers as low as n = 2, 3, a stable conformation similar to 3_1 helix of all-*trans* polyproline II (PLP II) [15, 16], and potential metallic [17–27] or radical Trp/Tyr [28–34], Met(S∴Br)/Trp [29] and Met(S∴Br)/Tyr [29, 35] D/A couples. Longer oligoproline bridges were also successfully used as spacers in the studies on distance dependence of electronic energy transfer [36]. The use of $Trp^{\bullet}$ radical in model systems was justified by the observation of an efficient intramolecular radical transformation $Trp^{\bullet} \rightarrow TyrO^{\bullet}$ in the pulse radiolysis studies on a number of proteins [37, 38], and by accumulating evidence that tryptophan and tyrosine radicals are involved in certain cellular enzymatic and light-driven electron transfer redox reactions [39–45].

In this review investigations on LRET in oligoproline bridged $Trp^{\bullet}$/Tyr systems [28–31] and between $Trp^{\bullet}$/Tyr pairs in hen egg-white lysozyme [46, 47], carried out under the author's guidance, will be summarized and discussed in relation to similar studies from other laboratories.

KINETICS OF $Trp^{\bullet} \rightarrow TyrO^{\bullet}$ TRANSFORMATION IN H-Trp-(Pro)$_n$-Tyr-OH PEPTIDES

The intramolecular one-electron redox reaction (2), involving electron transfer across an X = $(Pro)_n$ bridge from phenol group of tyrosine side chain to indolyl radical tryptophan side chain, was studied in neutral aqueous solution by the pulse radiolysis technique with the use of a linear electron accelerator and time-resolved spectrophotometric quantification of transient radical species [28–30]; the indole side chain of tryptophan was first (within $\leq 1\ \mu s$) selectively oxidized to $Trp^{\bullet}$ by neutral azide radicals, $N_3^{\bullet}$, and then first-order kinetics of $Trp^{\bullet}$ decay and simultaneous appearance of $TyrO^{\bullet}$ was measured.

$$Trp^{\bullet}\text{-X-TyrOH} \xrightarrow{k_{ET}} Trp[H]\text{-X-}TyrO^{\bullet} \quad (2).$$

The use of small electron doses per pulse for generation of $N_3^{\bullet}$ radicals and low concentration of the peptides eliminated interference

from a slow second-order radical decay and intermolecular radical transformation, respectively, and thus allowed determination of the first-order rate constants of reaction (2) with a reasonable accuracy.

Our first experiments on LRET in peptides with n = 1–3 [28, 29], supplemented subsequently for their longer analogues with n = 4, 5 [30], clearly demonstrated that the rate of the radical $Trp^{\bullet} \rightarrow TyrO^{\bullet}$ transformation decreases exponentially, in the first approximation, with the growing number n of Pro residues between terminal Trp and Tyr residues. This observation has soon been confirmed by the results of similar investigations on the same and an analogous group of peptides, with the reversed order of terminal residues: H-Tyr-$(Pro)_n$-Trp-OH, carried out in other laboratories [32–34]. The observed exponential dependence of the rate of intramolecular radical transformation in these peptides on the number of bridging proline units was in agreement with predictions of the theoretical electron tunneling model [4, 5], and thus proved involvement of LRET in reaction (2).* Moreover, it confirmed that oligoproline bridged systems are suitable models for studies on the distance dependence of LRET across an ordered single peptide pathway. A more detailed analysis of the dependence of k_{ET} on the number n of Pro residues indicated, however, that slopes of ln k_{ET} *vs.* n plots for shorter (n = 0–2) and longer (n = 3–5) peptides differ considerably (cf. Fig. 1). Thus, this observation pointed to involvement in shorter peptides, of a faster electron transfer, most probably through direct contacts between the aromatic rings of terminal amino acids. To rationalize these findings in terms of the theory of the distance dependence of LRET kinetics, separation distances and spatial disposition of the aromatic side chains in linear peptides studied had to be first evaluated from their conformational preferences and conformational dynamics. The commonly applied earlier practice to evaluate these distances in -$(Pro)_n$-bridged systems by assuming that, irrespective of the polymerization number n, they attain a regular structure resembling crystalline PLP II has been shown to be far from satisfactory [30, 48].

Conformation and conformational dynamics of H-Trp-$(Pro)_n$-Tyr-OH peptides

Conformational properties of H-Trp-$(Pro)_n$-Tyr-OH, n = 0–5, peptides were studied experimentally by ^1H and ^{13}C NMR [48, 49] and CD [16] spectroscopy, and theoretically by molecular mechanics and molecular dynamics modeling [30, 31, 48] with the help of AMBER 3.0 and/or 4.0 software. These properties were found to be governed by a number of interdependent equilibria (Fig. 2): (i) *trans* ↔ *cis* isomerization (ω dihedral angle) about

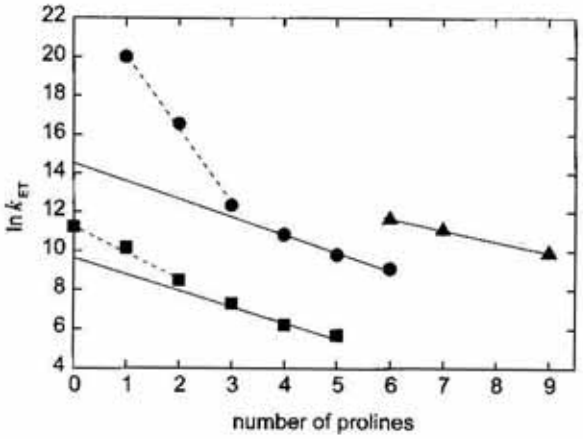

Figure 1. Bridge length dependence of the rate of LRET [31, 48]; plots of ln k_{ET} *vs.* number n of Pro residues for: (■) H-Trp-$(Pro)_n$-Tyr-OH, n = 0–5, series; (●) $[(bpy)_2Ru^{II}L(Pro)_nCo^{III}(NH_3)_5]^{4+}$, n = 0–6, series; (▲) $[(bpy)_2Ru^{II}L(Pro)_napy\text{-}Ru^{III}(NH_3)_5]^{4+}$, n = 6, 7, 9, series.

the X-Pro peptide bonds, (ii) rotation of Trp and Tyr side chains about C^{α}–C^{β} and C^{β}–C^{γ}

*In neutral aqueous solution the electron transfer is formally accompanied by a *net* proton transfer due to breakage of tyrosine O–H bond: $Tyr[OH] - e^- \rightarrow Tyr[O]^{\bullet} + H^+$, and formation of indole N–H bond: $Trp^{\bullet} + e^- \rightarrow Trp^-$; $Trp^- + H^+ \rightarrow Trp$, ($pK_a$ 16.8). Since O–H and N–H groups are involved in a very fast proton exchange with bulk water ($k \approx 10^{12}$ s^{-1}) the protonation/deprotonation equilibria accompanying electron transfer cannot be expected to limit the rate of the radical transformation reaction occurring on the microsecond time scale. An additional argument in support of this conclusion is that the mechanism of reduction of $Trp^{\bullet}$ and N-methylated tryptophan radical cation, $MeTrp^{\bullet}$ [34] is similar, in spite of the fact that reduction of the latter does not require protonation and thus the $MeTrp^{\bullet} \rightarrow TyrO^{\bullet}$ reaction does not involve a *net* proton transfer.

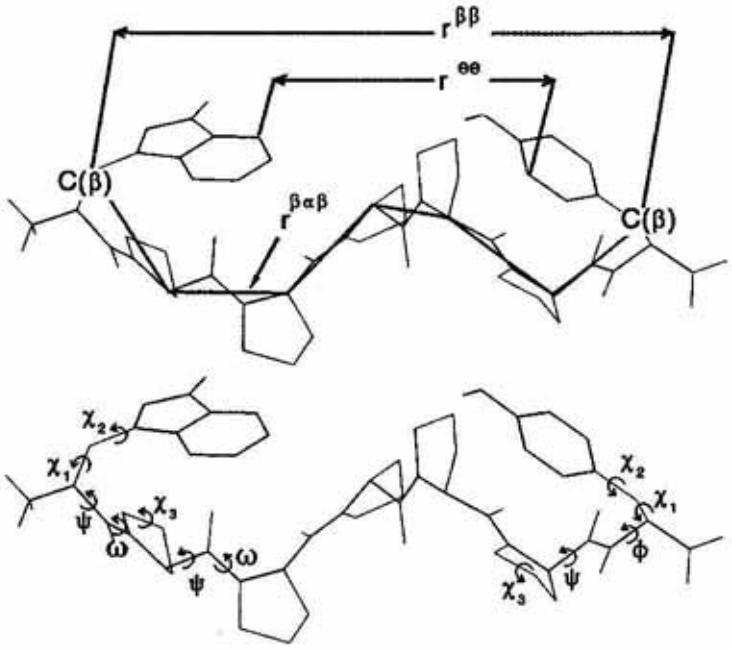

Figure 2. Structural scheme and definition of conformational parameters of H-Trp-(Pro)$_n$-Tyr-OH peptides [31, 48].

bonds (χ_1 and χ_2 dihedrals, respectively), (iii) extended helix ↔ poly-L-proline II (all-*trans* 3_1 helix) type conformation within the -(Pro)$_n$- bridge in peptides with n ≥ 2, (iv) β {ψ(Pro) angle ≈ 160°} ↔ α{ψ(Pro) ≈ 45°} within the Pro-Tyr fragment, and (v) *up* ↔ *down* conformations of the pyrrolidine Pro side chain (χ_3 angle).

Trans ↔ *cis* isomerization (i) proved to occur most readily at the Trp–Pro bond, so that populations of corresponding major isomers of zwitterionic forms of the peptides are comparable and constitute a 0.85–0.90 molar fraction of the total peptide content. The rate constant for interchange between these isomers at 298 K has been estimated to be close to 10^{-2} s^{-1}, that is 4–6 orders of magnitude slower than that observed for electron transfer reaction 2. Thus, in this reaction, the two isomers had to be treated as separate species.

Rotations (ii) of the Tyr side chain were found relatively free both in *trans* and *cis* isomers, with a marked preference for the $\chi_1(g-)$ rotamer in longer peptides. Rotations of Trp, however, appeared highly dependent on the configuration about the Trp–Pro bond. In *trans* isomers the indole ring rotates quite freely, while in *cis* form of all the peptides this rotation is severely restricted and this form is characterized by a high population (≈ 0.85) of the staggered $\chi_1(t)$ rotamer and $\chi_1(t)$, $\chi_2(-)$ conformation of the whole side chain. All these rotamers, with lifetimes in the time domain of 10^{-9}–10^{-12} s, exchange frequently during the life time of the $Trp^{\bullet}$ radical. In short-bridged peptides (n = 0–2), rotations of these side chains combined with oscillations of the backbone ψ angle lead to appearance of multiple low-energy conformers characterized by a close edge-to-edge approach of the indole and phenol rings.

Conformation of the -(Pro)$_n$- fragment was found to vary somewhat with the number of adjacent Pro residues. It assumes a PLP II -like helical conformation (ψ(Pro) angle in the β range) in *all-trans* isomers beginning with n = 3 and its conformational rigidity increases with the growing n, but even at n = 2 both Pro residues adopt backbone dihedral angles close to those of PLP II. Involvement of $\beta \leftrightarrow \alpha$ transitions at the ψ(Pro) angle, postulated by Sneddon & Brooks [50] on the basis of their CHARMM simulations of conformational dynamics of Pro peptides, proved insignificant in the light of our potential of mean force calculations for Trp-Pro, Pro-Pro and Pro-Tyr fragments [31, 48]. The calculated energy barriers between respective $\psi(\beta)$ and $\psi(\alpha)$ states and their corresponding lifetimes indicated that the mean life time of the $\psi(\alpha)$ state in Pro-Pro is about 6×10^{-6} s, so that a transient population of corresponding conformers of the -(Pro)$_n$- fragment with one Pro residue in this state can be expected to

be insignificantly low on the time scale of the observed electron transfer, and was therefore neglected.

On the other hand, $\beta \leftrightarrow \alpha$ transitions at the Pro residue preceding Tyr appeared much faster on the scale of electron transfer reaction 2, according to both NMR and molecular modeling studies, so that the corresponding local conformational states had to be included in calculations of low-energy conformers of the peptides.

The cyclic pyrrolidine side chains of Pro residues undergo very fast, ps, transitions between their *up* and *down* equilibrium conformations at the χ_3 angle, as shown both by NMR and molecular modeling.

In light of the described conformational dynamics of the H-Trp-$(Pro)_n$-Tyr-OH peptides in solution, proper parametrization of possible LRET pathways required their representation as ensembles of fast exchanging side chain and ψ(Pro-Tyr) backbone conformers of the major *cis* and *trans* isomers about the Trp–Pro bond, and -$(Pro)_n$- bridge in a PLP II type conformation.

Modeling of LRET pathways

Considering the outlined conformational properties of the peptides in connection with the characteristic two step dependence of experimental LRET rates on the number of bridging Pro residues, two molecular pathways for electron transfer could be reasonably envisaged: (i) through space (TS), *viz.* directly between the aromatic rings in van der Waals contact and/or mediated by water molecules of the solvation shell, and (ii) through the peptide backbone (TB). The corresponding distances for individual low-energy conformers (j) within each isomeric ensemble (i), r_{ij}, were consequently calculated for the TS pathway as edge-to-edge $r_{ij}(C^{ee})$ between carbon and other (N,O) atoms of the indole and phenol rings, and for the TB pathway, originally [30] as $r_{ij}(C^{\beta\beta})$, the shortest distance between C^β atoms of the terminal Trp and Tyr along the peptide backbone, or more recently [31, 48], as $r_{ij}(C^\beta C^\alpha C^\beta)$ between the C^β atoms of the terminal amino acids along a path joining the backbone C^α atoms (cf. Fig. 2). The latter parametrization follows a path of the highest electronic density of molecular orbitals and thus mimics better the TB electron transfer pathway.

The TS and TB distances were calculated for low-energy conformers the energies of which were higher by not more than 42 kJ mol^{-1} with respect to the lowest energy conformer within a given isomeric ensemble. Structures of these conformers were calculated for zwitterionic forms of the peptides with the use of AMBER 3.0 program in united atom parametrization and dielectric constant of 81 (to mimic an aqueous environment). For each peptide isomer with -$(Pro)_n$- bridge in the PLP II structure (adopted from X-ray diffraction data [51]), a set of 324 starting conformers, corresponding to all possible combinations of the N- and C-terminal side chain conformations, and β and α ψ(Pro-Tyr), was generated and subjected to further energy minimization. During the latter step

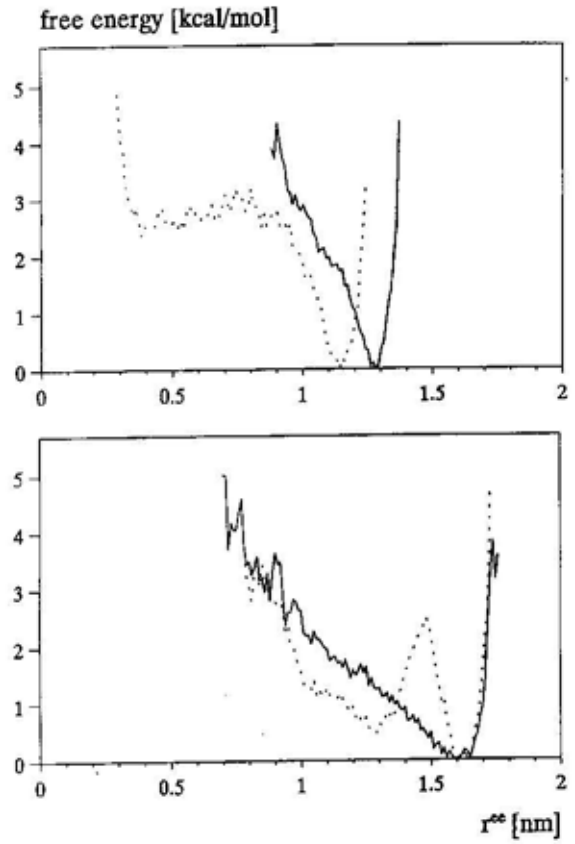

Figure 3. Free energy - r^{ee} profiles for *cis* (—) and *trans* (· · ·) isomers of H-Trp-$(Pro)_2$-Tyr-OH (top panel) and H-Trp-$(Pro)_3$-Tyr-OH peptides (bottom panel), obtained from 10 ns molecular dynamics simulations [31, 48].

all dihedral angles were allowed to vary. The ensembles of low-energy conformers thus obtained fairly well reproduced the main conformational features of the peptides and pointed to distinct differences between backbone conformations of n = 0–2 and n = 3–5 groups of peptides, as well as to the occurrence in the former group of multiple conformers with short contacts between the aromatic rings. Very similar distributions were obtained also from molecular dynamics simulations [31, 48]. The r^{ee}-free energy profiles for n = 2 and n = 3 derived therefrom (Fig. 3) are representative for the short- and long-bridged systems, respectively.

Therefore, our approach aimed at distinguishing which of the possible molecular pathways is actually involved in reaction 2, and at evaluation of the corresponding β descriptors of the exponential distance dependence of LRET. For this purpose, relative rate constants, k_{ij}, for LRET for individual conformers and of average values thereof for each peptide isomer $\langle k \rangle_i = \Sigma_{ij}\, k_{ij}\omega_{ij}$ (where ω_{ij} is the Boltzman probability of occurrence of a jth conformer of ith isomer) were calculated, and then the $\langle k \rangle_i$ values fitted to the experimental k_{ET} data with use of equation 3:

$$k = k_0 \exp\,[-\beta(r-r_0)] \qquad (3),$$

where k_0 is the rate constant at $r = r_0$, corresponding to the closest edge-to-edge approach of redox centers, and $\beta = \beta_{el} + \beta_n$ expresses electronic (β_{el}) and nuclear (β_n) contributions to the overall distance dependence of the rate k of LRET [4] according to a number of assumed models of LRET. Originally, four principal LRET models were probed [30]: (1 and 2) involving either the TB or the TS pathway, (3) the two pathways, TB + TS, simultaneously, and (4) the TB + TS *cos* Θ, in which the *cos* Θ function (Θ is the dihedral angle between the planes of indole and phenol rings) was introduced, as a rough account of the dependence of LRET along the TS pathway on the overlap between the π- and σ-orbitals of aromatic rings. Validity of the models was evaluated statistically with the use of an appropriate χ^2 distribution function. The best agreement between the experimental and calculated rates has been obtained for the last model (4) for the following values of the sought parameters: $\beta^{TB} = 2.8 \pm 0.4\ nm^{-1}$ and $\beta^{TS} = 120 \pm 40\ nm^{-1}$. The very high value of the β^{TS} parameter means that at $r_{ij}(C^{ee}) \approx 0.365$ nm the contribution to k_{ET} from the TS pathway practically vanishes to zero, so that TS-LRET takes place only in conformers with indole and phenol rings in close van der Waals contact. Since low-energy conformers of this type are dominant in short-bridged (n = 0–2) peptides, the TS pathway is competitive to the TB pathway only in this group. In longer peptides (n = 3–5), LRET takes thus place solely through the TB pathway, characterized by an unusually slow decay of electronic coupling between the $Trp^{\bullet}$ and Tyr redox centers, compared with those found for various electron transfer proteins [1, 2]: in photosynthetic reaction centers ($\beta = 14\ nm^{-1}$) and in metalloproteins ($\beta = 7\ nm^{-1}$).

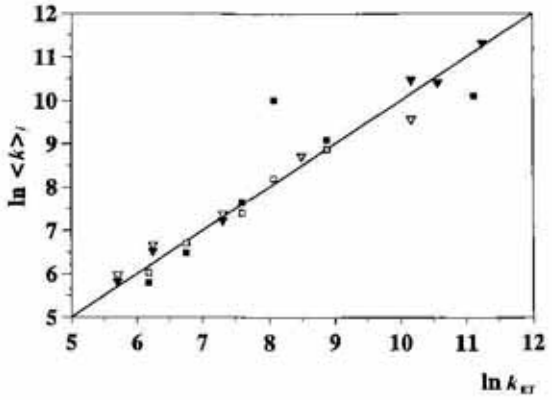

Figure 4. Correlation between the experimental, k_{ET}, and calculated best-fit rate constants of LRET, $\langle k \rangle_i$, for *cis* (open marks) and *trans* (filled marks) isomers of H-Trp-(Pro)$_n$-Tyr-OH (inverted triangles), and H-Tyr-(Pro)$_n$-Trp-OH (squares) peptides [31, 48].

More recently, overlap integrals, I_{DA}, between HOMO orbitals of the indolyl radical and phenol rings for all the low-energy conformers of the peptides were calculated [48], proportional to the H^2_{DA} matrix element in eqn. 1, and introduced in place of *cos* Θ function in calculation of adjustable parameters of eqn. 3. The calculated $\langle k \rangle_i$ values thus obtained exhibited very good agreement with the experimental k_{ET} data, as illustrated in

Fig. 4 by the plot of ln $\langle k \rangle_i$ *vs.* ln k_{ET}, for the following values of the sought parameters: $k_0^{TB} = (10 \pm 2) \times 10^4\ s^{-1}$, $\beta^{TB} = 2.5 \pm 0.1\ nm^{-1}$, and $k_0^{TS} = (14 \pm 2) \times 10^{12}\ s^{-1}$.

Using the same method we fitted also the calculated rates to the experimental k_{ET} data from Klapper and Faraggi laboratories for the same group of peptides [32, 33]. The results were qualitatively similar to those obtained with our k_{ET}'s. Moreover, we calculated also low-energy conformers for the series of peptides with the reversed order of terminal aromatic amino acids, H-Tyr-$(Pro)_n$-Trp-OH, and fitted the theoretical $\langle k \rangle_i$ values thus derived to the published experimental k_{ET} data [33] with the same set of adjustable parameters of the fitting function, as used in the case of H-Trp-$(Pro)_n$-Tyr-OH peptides. Again, an excellent agreement was obtained between the experimental and calculated LRET rate constants, as illustrated in Fig. 4. This finding demonstrated (i) that in the two linear peptide systems studied directional specificity of LRET does not occur, as it has been claimed earlier [33] on the basis of a difference observed between the slopes of ln k_{ET} *vs.* n plots, and (ii) the necessity of taking into account the conformational dynamics of such systems in interpretation of the distance dependence of LRET rates therein.

To confirm the validity of the two-pathway model of LRET in linear oligoproline bridged peptides reaction 2 has been recently studied (J. Poznański, K. Bobrowski, J. Holcman, M. Ciurak, J. Malicka & K.L.Wierzchowski, unpublished) also in a six-membered all-L cyclic peptide, c(-Gly-Trp-$(Pro)_2$-Tyr-Gly-), designed as a model system in which collisions between aromatic rings of Trp and Tyr should be sterically impossible. Indeed, ^1H NMR and molecular dynamics investigations demonstrated that this peptide in aqueous solution exhibited the conformational pattern depicted in Fig. 5, in which Pro_3 and Pro_4 proline residues occur in $\omega(trans)$ and $\omega(cis)$ configurations, respectively, and the distribution of edge-to-edge separating distances between the phenol and indole rings (Fig. 6) is peaked at 6 Å (0.6 nm) so that their shortest separation distance is larger than 4.5 Å (0.45 nm). At such distances quantum mechanically calculated I_{DA} overlap integrals between the one electron HOMO orbitals of indolyl radical and phenol rings are vanishingly small, so that the TS pathway practically does not contribute at all to the observed k_{ET}. The measured value of the latter, $k_{ET} = 1.6 \times 10^3\ s^{-1}$, proved comparable to that ($1.5 \times 10^3\ s^{-1}$) found for H-Trp-$(Pro)_3$-Tyr-OH [30], although the separation distance between C^β atoms of aromatic side chains in the former is shorter than in the

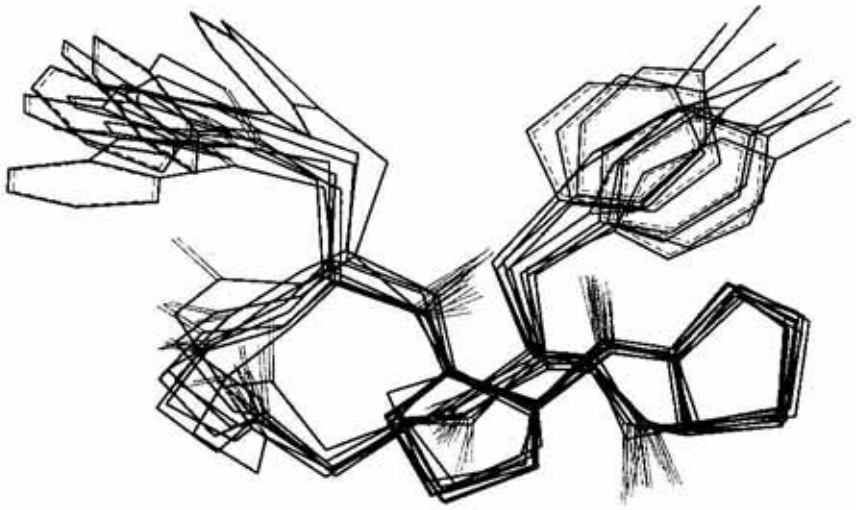

Figure 5. Superimposed structures of dominant c[-Gly-Trp-$(Pro)_2$-Tyr-Gly-] conformers: obtained from molecular dynamics modeling with NMR constrains (J. Poznański, unpublished).

latter system. This is probably due to a lower efficiency of LRET across the -Pro(*trans*)-Pro(*cis*) bridge in the cyclic peptide and to a small additional contribution to k_{ET} from LRET across the highly dynamic -$(Gly)_2$- bridge.

Effect of protonation of $Trp^{\bullet}$ radical

The neutral indolyl radical of tryptophan $Trp^{\bullet}$ remains in equilibrium with its protonated form, *viz.* tryptophan radical cation $TrpH^{\bullet+}$, pK_a for which was found to vary from 4.3 for the free amino acid up to about 5 in some dipeptides [52, 53]. Consequently, the effective redox potential of tryptophan radical is pH dependent and varies from 1.015–1.05 V at pH 7 for its neutral form [53, 54] to 1.15 V at pH 2 [54] for the protonated radical cation. Although only about 0.1 V separates $TrpH^{\bullet+}$ from $Trp^{\bullet}$, yet the reactivity of the former in simple one-electron bimolecular transfer reactions, including also tyrosine, was found to be by 1–2 orders of magnitude higher than that of the latter [52]. Redox potential of tyrosine is also pH dependent, owing to a large difference in electronic structure between phenol and phenolate side chains (pK_a 10.1). Consequently, the relative magnitude of redox potentials for tryptophan and tyrosine shows a marked pH dependence [54], as does also the efficiency and direction of electron transfer between them: tyrosine radicals have been predicted to be able to oxidize tryptophan at pH < 3 and at pH > 12. Indeed, the last reaction was observed in peptide bridged Trp/Tyr systems [29, 55]. It was therefore of interest to study also the pH dependence of reaction 2 in the acidic pH range where $Trp^{\bullet}$ and $TrpH^{\bullet+}$ forms of tryptophan radical remain in equilibrium. Our preliminary experiments at pH 4 [29] on oligoproline bridged (n = 0–3) Trp/Tyr peptides indicated that the rate of LRET under these conditions was remarkably higher than at neutral pH. More recently, the effect of $Trp^{\bullet}$ protonation on the rate of intramolecular LRET in H-Trp-$(Pro)_n$-Tyr-OH peptides, n = 4 and n = 5, has been studied over a broad pH range of 2–6 (K. Bobrowski, J. Holcman & K.L. Wierzchowski, unpublished), by the pulse radiolysis technique with the use of $Br_2^{\bullet-}$ anion radical which selectively oxidizes Trp species. In the whole pH range studied only $Trp^{\bullet}/TrpH^{\bullet+} \rightarrow TyrO^{\bullet}$ first-order radical conversion was observed, the rate of which sigmoidally increased by a factor of 60 between pH 6 and 2. The experimental k_{ET} *versus* pH data were found to be related by a function of the form: $k_{ET} = k(TrpH^{\bullet+})/(1 + K_a/[H^+])$, wherefrom pK_a 4.1 ± 0.05 for $TrpH^{\bullet+}$ dissociation was determined. The uniform direction and mechanism of the electron transfer reaction observed in both peptides up to pH 2 is at variance with the earlier Harriman's prediction [54] that below pH 3 $TyrO^{\bullet}$ should oxidize Trp to $Trp^{\bullet}/TrpH^{\bullet+}$. The pH dependence

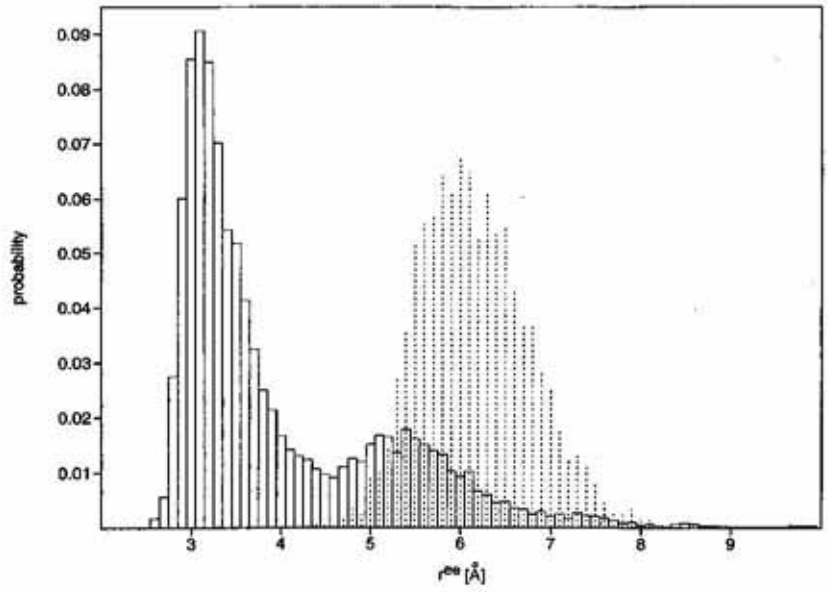

Figure 6. Distribution of the edge-to-edge distances between indole and phenol rings obtained from molecular dynamics simulation for c[-Gly-Trp-(Pro)$_2$-Tyr-Gly-] (dashed lines) and H-Trp-(Pro)$_2$-Tyr-OH (rectangles) peptides (J. Poznański, unpublished).

of redox potentials of Trp and Tyr in proline-bridged peptides seems thus to be different from those measured for free amino acids, and should be subjected to further investigations. The 0.1 V difference between redox potentials of $Trp^{\bullet}$ and $TrpH^{\bullet+}$ [54, 55] is too small to explain in terms of the LRET theory (eqn.1) the 60-fold higher $k(TrpH^{\bullet+})$ rate constant for one electron oxidation of Tyr. Conformation of both oligoproline-bridged peptides was shown by CD spectrophotometry to remain the same over the whole 2–6 pH range (K. Majcher & K.L.Wierzchowski, unpublished). Also the I_{DA} overlap integral between HOMO orbitals of phenol and neutral and protonated indolyl radical rings were found closely similar (J. Poznański, unpublished). Therefore, the 60-fold lower $k_{ET}(Trp^{\bullet})$ relative to $k(TrpH^{\bullet+})$ can be attributed in part to a larger value of the outer part, λ_{out}, of reorganization energy, (required for reorientation of solvent molecules around DA pair in the transition state), expected for the neutral form of the Trp indolyl radical. A similar explanation has been proposed earlier to explain the 1–2 orders of magnitude higher electron transfer rates of the radical cation of free tryptophan [52] and the main contribution to the higher value of λ_{out} was sought in a large entropy loss originating from the requirement for protonation in the transition state of the incipient tryptophan anion, Trp^{-} (for indole ring deprotonation pK_a 16.8), formed upon electron addition to $Trp^{\bullet}$. Such explanation finds additional support from the studies on reaction 2 in H-$MeTrp^{\bullet+}$-$(Pro)_n$-Tyr-OH model system [34]. In this system, $MeTrp^{\bullet+}$ cation radical upon electron addition forms instantanously neutral MeTrp (addition of H^+ is not required), so that λ_{out} is expected to be close to that for $TrpH^{\bullet+}$. Indeed, the corresponding rate constant for LRET in n = 3 peptide, $k_{ET} = 2.1 \times 10^4\ s^{-1}$ [34], is by one order of magnitude higher than that found for $Trp^{\bullet}$ reduction by Tyr in the analogous peptide [30].

In all the three oligoproline-bridged redox systems bearing $Trp^{\bullet}$/Tyr, $TrpH^{\bullet+}$/Tyr and $MeTrp^{\bullet+}$/Tyr couples, the distance dependence of the rate of LRET was found quite similar.

This indicates that it is rather the electronic structure of the peptide bridge than the magnitude of electron coupling between donor and acceptor centers which determines the decay of the amplitude of electron wavefunction along the LRET pathway. Comparison of kinetic LRET data for the $Trp^{\bullet}$/Tyr redox pair with those for intramolecular electron transfer across the same -$(Pro)_n$- bridge between liganded (ammine and bipyridine ligands) metallic Ru^{II}/Co^{III}, Os^{II}/Ru^{III} or Os^{II}/Co^{III} donor-acceptor pairs in appropriately derivatized oligoproline peptides with polymerization number ranging up to n = 9 [21, 24], adds strong support to the last conclusion. The plots of $\ln k_{ET}$ *vs.* the donor-acceptor separation distance (the number n of Pro residues in the bridge), approximated by two component linear plots with different slopes for short-bridged and longer-bridged peptides (cf. Fig. 1), point to a general similarity between the two systems. While the slopes for short-bridged $Trp^{\bullet}$/Tyr and metallo systems differ considerably, those for long-bridged peptides are very similar (β descriptors of 2.5 [31, 48] and 3.0 nm^{-1} [21], respectively). The steeper slopes for short-bridged peptides are due to a fast decay with growing n of the number of conformers with close contacts between the terminal D/A pairs and thus contribution from the TS pathway to the observed k_{ET}, while the large difference between the slopes for $Trp^{\bullet}$/Tyr and metallo pairs reflects the larger size of the latter relative to the former [30, 31]. Low and similar values of β coefficients for longer peptides provide a strong argument in favour of a high electron transferability of the helical PLP II type conformation of the -$(Pro)_n$- bridges and its independence of the nature of the attached D/A pair. On theoretical grounds [56], the dependence of β on the nature of electron-donor pair could appear only when the energy of the tunneling electron would be close to the energy of atomic orbitals of the intervening bridge. This is apparently not the case in the systems in question.

It would be of great interest to compare electron transferability of the 3_1-helical PLP II type and α-helical single polypeptide pathways. Unfortunately, attempts to charac-

terize distance dependence of kinetics of LRET across an α-helical bridge failed so far [24, 57, 58], owing to low thermodynamic stability of short α-helices and/or dominance of TS pathways.

$Trp^{\bullet} \rightarrow TyrO^{\bullet}$ TRANSFORMATION IN HEN EGG-WHITE LYSOZYME

The intramolecular $Trp^{\bullet} \rightarrow$ Tyr transformation was observed in a group of proteins [37, 38] including also hen egg-white lysozyme (HEWL). The main rationale underlying these early pulse radiolysis studies was to elucidate how such a long-range unpaired electron transfer may extend the target size for radiation-induced damage to sub-cellular protein systems [59]. Nowadays, well documented participation of $Trp^{\bullet}$ and $TyrO^{\bullet}$ radicals in a number of cellular redox reactions adds a new dimension to this rationale and makes further studies on LRET involving $Trp^{\bullet}$/Tyr redox couple in proteins worth continuing. The well known structure and conformational dynamics of hen egg-white lysozyme prompted us [46, 47] and the group of Klapper and Faraggi [60] to choose this protein as a good model for such studies.

The main goal of our studies was to identify which of the potential $Trp^{\bullet}$/Tyr redox pairs, formed by six tryptophan and three tyrosine residues present in HEWL, and which of the associated LRET pathways are actually involved in the observed $Trp^{\bullet} \rightarrow TyrO^{\bullet}$ radical transformation. Our preliminary pulse radiolysis study on the temperature dependence of kinetics of LRET in HEWL [46] showed a close similarity between the Arrhenius plots for the kinetics of this process and the specific enzymatic reaction of HEWL, suggesting that similar thermally induced conformational fluctuations are involved in activation of both these processes in this protein. Three highly solvent-accessible residues Trp62, Trp63 and Trp123, known to be involved in the binding of oligosaccharide-type substrates, were expected to be most susceptible to oxidation by $N_3^{\bullet}$ radicals [60]. Trp62 was found also selectively oxidizable by ozone to N′-formylkynurenine (NFKyn) [61, 62]. Taking advantage of this knowledge, our approach to identification which of the potential $Trp^{\bullet}$/Tyr redox pairs in HEWL are actually involved in LRET combined determination by pulse radiolysis of the rate constants of LRET and radical yields (G) for: (i) the native enzyme, (ii) its complex with an oligosaccharide inhibitor — triacetyl-chitotriose, HEWL$(GlcNAc)_3$, and (iii) the selectively oxidized by ozone NFKyn62-HEWL derivative. The parameters of LRET were determined in function of pH and temperature so as to perturb the structure of HEWL in a controled and known way.

The reaction was induced by selective oxidation of Trp with $N_3^{\bullet}$ radicals under low concentration of the reactants but at a high HEWL/$N_3^{\bullet}$ molar ratio, so that more than 99% of the oxidized protein molecules contained only a single tryptophyl radical. Synchronous decay of $Trp^{\bullet}$ and build up of $TyrO^{\bullet}$ conformed satisfactorily to first-order kinetics, indicating that LRET involved either one or more $Trp^{\bullet}$/Tyr redox pairs characterized by similar rate constants. The rate constant of LRET, k_{ET}, was found to increase with decreasing pH (Fig. 7) showing the following characteristics: (i) in the pH range of 7.4–5.2 the plot of k_{ET} *vs.* pH was sigmoidal, reflecting protonation of Glu35 ($pK_a \approx 6$) and pointing to involvement of a conformational control of the kinetics of LRET, (ii) below pH 5.2 a sharp increase in the rate was observed due to the protonation of $Trp^{\bullet}$ to form $TrpH^{\bullet+}$ which oxidizes tyrosine faster than does $Trp^{\bullet}$ (see infra). Arrhenius plots of the temperature dependence of k_{ET} (Fig. 8) showed that the activation energy of LRET varies both with temperature and the state of the enzyme protonation. The activation energies were found in the range of 7.6–56.0 kJ mol^{-1} and were similar to those for activation of amide hydrogen exchange in native HEWL below its denaturation temperature [63–65]. Selective oxidation by ozone of the Trp62 indole side chain in HEWL to *N′*-formylkynurenine caused a large drop in the initial yield of $Trp^{\bullet}$ radicals, $G(Trp^{\bullet})_i$ in NFKyn62-HEWL. This was accompanied by a relatively small decrease in k_{ET} but selective oxidation by ozone had a pronounced effect on its temperature dependence. Taken together these observations indicate that, of the six trypto-

phans present in HEWL, Trp62 contributes about 50% to the yield of the observed LRET. In the enzyme-inhibitor complex, HEWL-$(GlcNAc)_3$, where Trp62 and Trp63 are known to be completely shielded from the solvent by the bound triacetylchitotriose [66, 67], $G(Trp^{\bullet})_i$ was lower than in NFKyn62-HEWL, and both the kinetic and energetic characteristics of LRET at pH 5.2 were again somewhat different than in free HEWL. Considering known solvent accessibilities of tryptophans in the complex, the observed LRET process in HEWL$(GlcNAc)_3$ could be assigned to Trp123.

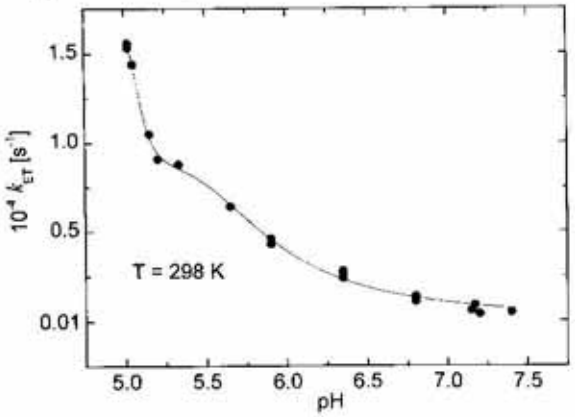

Figure 7. Dependence of the rate constant of LRET on pH in native HEWL [47].

All these findings allowed us to conclude that in native HEWL the three most solvent accessible tryptophans: Trp62, Trp63 and Trp123 are simultaneously involved in LRET. Moreover, their electronic coupling with respective Tyr donor centers should be similar, since the overall rate of their reduction by coupled Tyr residue(s) could be well approximated as a single first-order process.

To evaluate which of the three tyrosine residues present in HEWL: Tyr20, Tyr23 or Tyr53, form effective $Trp^{\bullet}$/Tyr redox couples with one or more of the three Trp residues implicated in LRET and can thus be expected to contribute significantly to the observed k_{ET}'s, we applied the PATHWAYS model [68, 69]. So far this model was successfully applied to predict the relative rates of electron transfer in a number of ruthenium derivatized redox proteins of known three-dimensional structure [1, 7, 70]. In this model, a single electron tunneling pathway is defined as a combination of interacting bonds that link a donor (D) with an acceptor (A) *via* a combination of covalent (C), hydrogen bonded (H) and/or van der Waals through-space (S) connections. The donor-acceptor electronic coupling for such a pathway, T_{DA}, is approximated as a product of the decay factors, ε, corresponding to all interacting bonds: $\Pi_i\ \varepsilon^C{}_i\ \Pi_i\ \varepsilon^H{}_i\ \Pi_i\ \varepsilon^S{}_i$. These unitless factors are appropriately parametrized. Each decay factor is associated with an effective distance: $d_{eff} = -\log \varepsilon$. Using graph theory the program searches for the shortest effective distance between donor and acceptor within a known protein network of bonded and nonbonded contacts. We applied essentially the original parametrization of the decay factors from the standard database. For C–C bonds in aromatic rings with delocalized wave functions (Trp,Tyr, Phe) a new parametrization, $\varepsilon^C = 0.95$, was introduced, for a better account for their lower electron transfer damping (J. Poznański, unpublished). The starting crystallographic coordinates for the protonated form of triclinic HEWL [71] were taken from the Brookhaven Protein Data Bank (entry 2LZT).

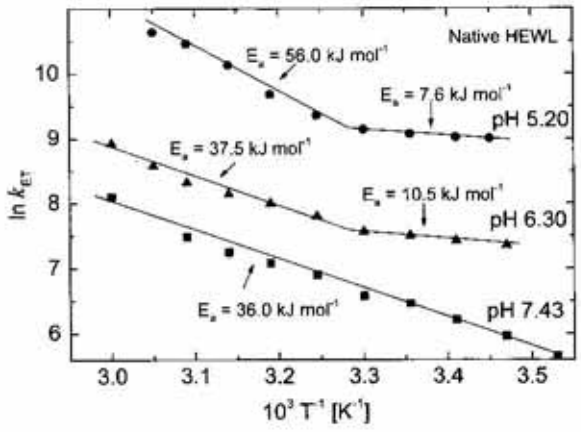

Figure 8. Arrhenius plots for the temperature dependence of the rate constant, k_{ET}, of LRET for native HEWL at the pH values indicated [47]; E_a are the corresponding energies of activation, derived from the slopes of the plots.

The calculated couplings corresponding to these pathways, collected in Table 1, indicate that the most strongly coupled $Trp^{\bullet}$/Tyr pairs are those which include Trp residues deeply buried in the so called „hydrophobic box" of HEWL, and thus are practically inaccessible to azide radical attack: Trp111 and

Table 1. Dominant electron-transfer pathways between potential Trp/Tyr donor/acceptor pairs in hen egg-white lysozyme, calculated according to the PATHWAYS model [47]

Donor	Acceptor	*Pathway	#Distance [nm]	T_{DA}
Tyr23	Trp62	-(S)-Val99-(C)-Ile98-(S)-Trp63-(C)-	3.59	4.83 exp(-07)
Tyr53	Trp123	-(C)-Gly54-(C)-Ile55-(S)-Ser36-(H)-Ala32-(C)-Lys33-(S)-	3.55	1.39 exp(-06)
Tyr20	Trp62	-(S)-Lys96-(C)-Lys97-(S)- Trp63-(C)-	3.15	1.59 exp(-06)
Tyr53	Trp111	-(H)-Gln57-(C)-Leu56-(H)-Trp108-(S)-	3.14	5.72 exp(-06)
Tyr20	Trp123	-(S)-Trp28-(C)-Val29-(S)-	2.95	5.91 exp(-06)
Tyr53	Trp28	-(H)-Gln57-(C)-Leu56-(H)-Trp108-(S)-	3.29	1.85 exp(-05)
Tyr23	Trp63	-(S)-Val99-(C)-Ile98-(S)-	2.36	3.19 exp(-05)
Tyr23	**Trp123**	-(S)-Trp111-(S)-Cys115-(S)-Cys30-(H)-	**2.10**	**7.52 exp(-05)**
Tyr20	Trp63	-(S)-Lys96-C-Lys97-(S)-	2.14	9.45 exp(-05)
Tyr20	Trp111	-(S)-Tyr23-(S)-	2.49	2.36 exp(-04)
Tyr53	**Trp62**	-(S)-Ser60-(C)-Arg61-(C)-	**2.10**	**3.69 exp(-04)**
Tyr53	**Trp63**	-(S)-Ser60-(C)-Asn59-(S)-	**1.70**	**5.68 exp(-04)**
Tyr20	Trp108	-(S)-Val99-(S)-	1.90	7.55 exp(-04)
Tyr53	Trp108	-(H)-Gln57-(C)-Leu56-(H)-	1.86	9.79 exp(-04)
Tyr23	Trp108	-(H)-Met105-(S)-	1.31	5.20 exp(-03)
Tyr20	Trp28	-(S)-	1.21	1.08 exp(-02)
Tyr23	Trp28	-(S)-	0.99	2.67 exp(-02)
Tyr23	Trp111	-(S)-	1.03	3.90 exp(-02)

*Intervening amino-acid residues and types of connecting bonds: (C)-covalent, (H)-hydrogen, and (S)-through space van der Waals contact; Cys115 and Cys30 are linked by a disulfide bridge. #From OH of Tyr phenol to $N^{\varepsilon 1}$ of Trp indole.

Trp28, and Trp108 of the substrate binding cleft. The next strongly coupled group of the redox pairs includes the most solvent accessible Trp62 and Trp63, located on the surface of the substrate binding cleft, and Trp123 on the opposite side of the protein surface, the involvement of which in the observed LRET was directly demonstrated (Trp62) or indirectly implicated (Trp63,Trp123). Trp62 and Trp63 are coupled only to Tyr53 along the pathways depicted in Fig. 9. The rate constants of LRET along these pathways, proportional to the square of the electronic coupling, should not differ by more than a factor of about 2. Trp63 is also coupled to Tyr20 and Tyr23, but with a much lower strength so that the corresponding rates of LRET should be more than by two orders of magnitude lower than that of the Trp63/Tyr53 pair. The Trp123/Tyr23 pair is characterized by an electronic coupling of intermediate strength between the former two (cf. Table 1) along a pathway which includes 3 through-space electron jumps (cf. Fig. 9). The rate of LRET between the members of this pair can thus be expected to be considerably slower.

The results of the theoretical evaluation of the electronic coupling between various Trp/Tyr potential redox pairs in HEWL provided, thus, strong support to the conclusions derived from experimental data concerning involvement of Trp62 and Trp63 in LRET and the similarity of the rate constants for LRET between the Trp62/Tyr53 and

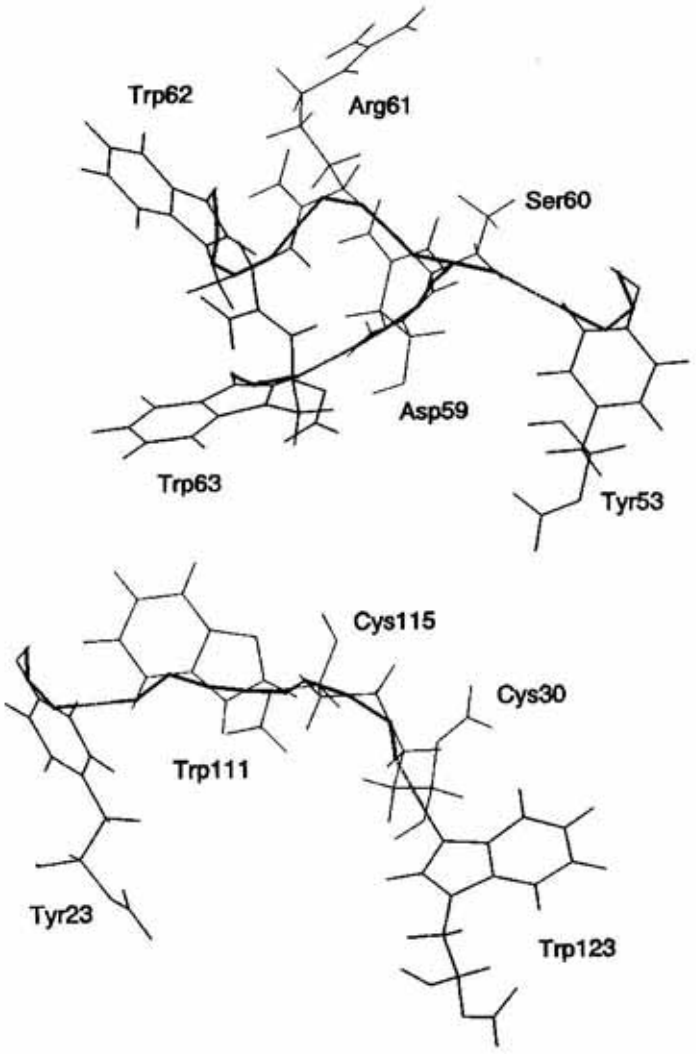

Figure 9. The dominant LRET pathways between Trp62/Tyr53, Trp63/Tyr53 and Trp123/Tyr23 potential donor-acceptor couples in native HEWL, selected with help of the PATHWAYS model [47]; light full lines — skeletons of amino-acid residues indicated, bold full lines — tunnelling of electron through peptide backbone covalent bonds, dashed lines — through-space electron jumps between atoms in van-der-Waals contacts.

Trp63/Tyr53 couples. They did not support, however, the postulated involvement of the Trp123/Tyr23 couple.

The values of the electronic coupling calculated for the dominant pathways between the redox centers in question were obtained for the static crystal structure of HEWL. Since the present version of the PATHWAYS model does not take into account dynamics of protein structure, electronic couplings for pathways involving a number of through-space jumps could be severely underestimated. This point of view finds support in the results of molecular dynamics studies on variation in time of distances between atoms involved in through-space electron jumps and, calculated therefrom, time dependence of the square of the electronic coupling, T^2_{DA}, for selected LRET pathways in question (J. Poznański, unpublished). In general, these results showed that variation of T^2_{DA}, governed for the most part by the presence of through-space electron jumps along a pathway, increases by approximately one order of magnitude per each jump. Evolution in time of the normalized value of T^2_{DA} for the Tyr23...Trp123 pathway (Fig. 10) indicates that a

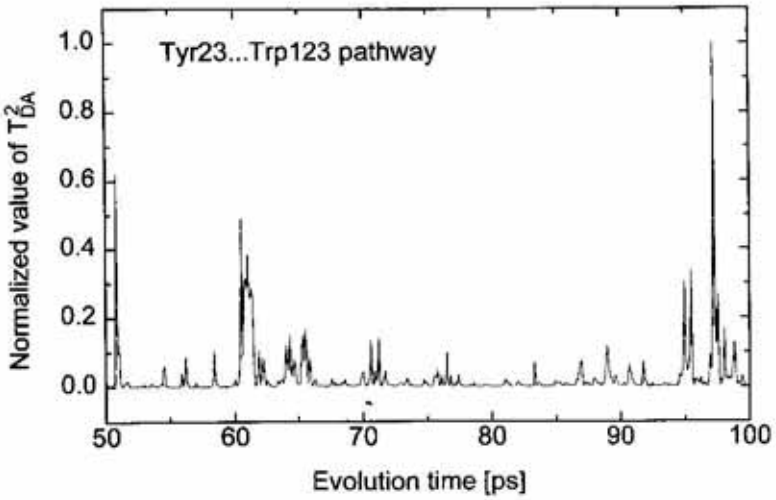

Figure 10. Variation in time of the square of the electronic coupling T^2_{DA} (normalized to its maximum momentary value) for the Tyr23...Trp123 dominant LRET pathway in HEWL [47]; time averaged value of the parameter equals 0.03, and median value is 0.0044.

very low time-averaged value of this parameter, corresponding to 0.03 of the maximal T^2_{DA} value (median: 0.0044) may occasionally attain a much higher momentary value. The results obtained indicate that electron transfer is strongly coupled to thermal motions of the protein matrix, so that any interpretation of LRET kinetics based on the static protein structure can be considered, at best, as semi-quantitative. This conclusion finds strong support in the most recent theoretical studies on the effect of protein dynamics on biological electron transfer (cf. [72] and references cited therein).

Finally, it is worth to discuss shortly implications emerging from the reviewed experimental investigations for the nature of conformational control of LRET in HEWL. This control was postulated on the basis of (i) the much larger energy of activation for reaction 2 in HEWL at neutral pH compared with that for the analogous reaction across the oligoproline bridge in Trp-$(Pro)_n$-Tyr peptides [29, 30], and (ii) its variation with temperature in the protonated form of HEWL. Temperature studies on the kinetics of hydrogen exchange in HEWL [63–65] have identified the occurrence of two distinct mechanisms for exchange, one (i) characterized by a high activation energy of the order of 400 kJ mol^{-1} directly associated with the cooperative thermal unfolding of the protein, and the second one (ii) of lower activation energy associated with local fluctuations in the protein structure. The activation energies for indole NH hydrogen exchange, consistent with the second mechanism, are about 55 kJ mol^{-1} for Trp63 and much below this value for Trp62 [64] and are very close to those determined for LRET in HEWL. It seems thus very probable that conformational fluctuations involved in activation of hydrogen exchange in HEWL contribute also to activation of LRET between $Trp^{\bullet}$/Tyr redox pairs in this protein. The very low value of E_a = 7.6 kJ mol^{-1}, ascribed to fluctuation of Trp62 in the protonated form of HEWL, is very close to that found in longer peptides of the H-Trp-$(Pro)_n$-Tyr-OH group [30]: 8 and 7 kJ mol^{-1} for n = 4 and n = 5 peptides, respectively. Such a low energy of activation is thus characteristic of practically free motions of a Trp indolyl side chain [73]. The observed variation with temperature of the activation energy of LRET in HEWL at pH values below 7.4 seems to be connected with the presence of multiple forms of protonated HEWL molecules, the contribution of particular species in the total population of HEWL molecules being pH-dependent.

In general, it can be expected that thermally induced local fluctuations in a protein matrix may modify the magnitude of electronic coupling between a donor-acceptor pair by allowing the intervening peptide backbone and the pair itself to attain a more or less favourable conformation for maximal overlap of the bridging atomic and molecular electron orbitals. These fluctuations should have a particularly strong influence on through-space couplings between non-bonded and hydrogen-bonded atoms, as shown by our dynamic simulation of variation in time of the square of electronic coupling along pathways including a different number of non-bonded connections.

The author wishes to express his gratitude and thanks to all collaborators and colleagues who over the years contributed in many ways to the pursued together studies referred to in this review.

REFERENCES

1. Gray, H.B. & Winkler, J.R. (1996) Electron transfer in proteins. *Annu. Rev. Biochem.* **65**, 537–561.
2. Moser, C.C., Keske, J.M., Warncke, K., Farid, R.S. & Dutton, P.L. (1992) Nature of biological electron transfer. *Nature* **355**, 796–802.
3. Marcus, R.A. (1993) Electron transfer reactions in chemistry — Theory and experiment (Nobel Lecture). *Angew. Chem. Intern. Edit. Engl.* **32**, 1111–1121.
4. Marcus, R.A. & Sutin, N. (1985) Electron transfers in chemistry and biology. *Biochim. Biophys. Acta* **811**, 265–322.
5. Hopfield, J.J. (1974) Electron transfer between biological molecules by thermally acti-

vated tunneling. *Proc. Natl. Acad. Sci. U.S.A.* **71**, 3640–3644.

6. Newton, M.D. (1991) Quantum chemical probes of electron-transfer kinetics: The nature of donor-acceptor interactions. *Chem. Rev.* **91**, 767–792.

7. Onuchic, J.N., Beratan, D.N., Winkler, J.R. & Gray, H.B. (1992) Pathway analysis of protein electron-transfer reactions. *Annu. Rev. Biophys. Biomol. Struct.* **21**, 349–377.

8. Skourtis, S.S. & Beratan, D.N. (1997) High and low resolution theories of protein electron transfer. *J. Biol. Inorg. Chem.* **2**, 378–386.

9. Prütz, W.A. & Land, E.J. (1979) Charge transfer in peptides. Pulse radiolysis investigation of one-electron reactions in dipetides of tryptophan and tyrosine. *Int. J. Radiat. Biol.* **36**, 513–520.

10. Prütz, W.A., Land, E.J. & Sloper, R.W. (1981) Charge transfer in peptides. *J.C.S. Faraday Trans. I* **77**, 281–292.

11. Prütz, W.A., Siebert, F., Butler, J., Land, E.J., Menez, A. & Garestier, T.M. (1982) Charge transfer in peptides. Intramolecular radical transformations involving methionine, tryptophan and tyrosine. *Biochim. Biophys. Acta* **705**, 139–149.

12. Prütz, W.A., Butler, J. & Land, E.J. (1983) Phenol coupling initiated by one-electron oxidation of tyrosine units in peptides and histone. *Int. J. Radiat. Biol.* **44**, 183–196.

13. Prütz, W.A., Butler, J. & Land, E.J. (1985) Methionyl-tyrosyl radical transition initiated by Br-2 in peptide model systems and ribonuclease A. *Int. J. Radiat. Biol.* **47**, 149–156.

14. Prütz, W.A., Butler, J., Land, E.J. & Swallow, A.J. (1986) Unpaired electron migration between aromatic and sulphur peptide units. *Free Radical Res. Commun.* **2**, 69–75.

15. Helbecque, N. & Loucheux-Lefebvre, M.H. (1982) Critical chain length for polyproline-II structure formation in H-Gly-(Pro)n-OH. *Int. J. Peptide Protein Res.* **19**, 94–101.

16. Wierzchowski, K.L., Majcher, K. & Poznański, J. (1995) CD investigations on conformation of H-X-$(Pro)_n$-Y-OH peptides (X=Trp,- Tyr; Y=Tyr,Met); models for intramolecular long range electron transfer. *Acta Biochim. Polon.* **42**, 259–268.

17. Isied, S.S. & Vassilian, A. (1984) Electron transfer across polypeptides. 3. Oligoproline bridging ligands. *J. Am. Chem. Soc.* **106**, 1732–1736.

18. Isied, S.S., Vassilian, A., Magnuson, R. & Schwartz, H.A. (1985) Electron transfer across polypeptides. 5. Rapid rates of electron transfer between Os(II) and Co(III) in complexes with bridging oligoprolines and other polypeptides. *J. Am. Chem. Soc.* **107**, 7432–7438.

19. Isied, S.S., Vassilian, A., Wishart, J.F., Creutz, C. & Schwartz, H.A. (1988) The distance dependence of intramolecular electron transfer rates: Importance of the nuclear factor. *J. Am. Chem. Soc.* **110**, 635–637.

20. Vassilian, A., Wishart, J.F., Hemelryck, B., Schwartz, H. & Isied, S.S. (1990) Electron transfer across polypeptides. 6. Long-range electron transfer in osmium-ruthenium binuclear complexes bridged with oligoproline peptides. *J. Am. Chem. Soc.* **112**, 7278–7286.

21. Isied, S.S., Ogawa, M.Y. & Wishart, J.F. (1992) Peptide-mediated intramolecular electron transfer: Long range distance dependence. *Chem. Rev.* **92**, 381–394.

22. Ogawa, M.Y., Wishart, J.F., Young, Z., Miller, J.R. & Isied, S.S. (1993) Distance dependence of intramolecular electron transfer across oligoprolines in $[(bpy)_2Ru^{II}\text{-L-}(Pro)_n\text{-}Co^{III}(NH_3)_5]^{3+}$, n = 1–6: Different effects for helical and nonhelical polyproline II structures. *J. Phys. Chem.* **97**, 11456–11463.

23. Ogawa, M.Y., Moreira, I., Wishart, J.F. & Isied, S.S. (1993) Long range electron transfer in helical polyproline II oligopeptides. *Chem. Phys.* **176**, 589–600.

24. Isied, S.S., Moreira, I., Ogawa, M.Y., Vassilian, A., Arbo, B. & Sun, J. (1994) New perspectives on long-range electron transfer in conformationally organized peptides and electron-transfer proteins: An experimental approach. *J. Photochem. Photobiol., A: Chem.* **82**, 203–210.

25. Schanze, K. & Sauer, K. (1988) Photoinduced intramolecular electron transfer in peptide

bridged molecules. *J. Am. Chem. Soc.* **110**, 1180–1186.

26. Schanze, K.S. & Cabana, L.A. (1990) Distance dependence of photochemical electron transfer across peptide spacers. *J. Phys. Chem.* **94**, 2740–2743.

27. Cabana, L.A. & Schanze, K.S. (1990) Photoinduced electron transfer across peptide spacers; in *Electron Transfer in Biology and the Solid State* (Johnson, M.K., King, R.B., Kurtz, D.M., Jr., Kutal, C., Norton, M.L. & Scott, R.A., eds.) pp. 101–123, American Chemical Society, Washington, D.C.

28. Bobrowski, K., Wierzchowski, K.L., Holcman, J. & Ciurak, M. (1987) Intramolecular charge transfer between tryptophan and tyrosine in peptides with bridging prolines. *Studia biophysica* **122**, 23–28.

29. Bobrowski, K., Wierzchowski, K.L., Holcman, J. & Ciurak, M. (1990) Intramolecular electron transfer in peptides containing methionine, tryptophan and tyrosine: A pulse radiolysis study. *Int. J. Radiat. Biol.* **57**, 919–932.

30. Bobrowski, K., Holcman, J., Poznanski, J., Ciurak, M. & Wierzchowski, K.L. (1992) Pulse radiolysis studies of intramolecular electron transfer in model peptides and proteins. 5. $Trp^{\bullet}$ - $Tyr^{\bullet}$ radical transformation in H-Trp-$(Pro)_n$-Tyr-OH series of peptides. *J. Phys. Chem.* **96**, 10036–10043.

31. Bobrowski, K., Poznański, J., Holcman, J. & Wierzchowski, K.L. (1998) Long range electron transfer between proline-bridged aromatic amino acids; in *Photochemistry and Radiation Chemistry* (Nocera, D.G. & Wishart, J.F., eds.) pp. 131–143, American Chemical Society,Washington, DC. (in presss).

32. Faraggi, M., DeFelippis, M.R. & Klapper, M.H. (1989) Long-range electron transfer between tyrosine and tryptophan in peptides. *J. Am. Chem. Soc.* **111**, 5141–5145.

33. DeFelippis, M.R., Faraggi, M. & Klapper, M.H. (1990) Evidence for through-bond long-range electron transfer in peptides. *J. Am. Chem. Soc.* **112**, 5640–5642.

34. Mishra, A.K., Chandrasekar, R., Faraggi, M. & Klapper, M.H. (1994) Long-range electron transfer in peptides. Tyrosine reduction of the indolyl radical: Reaction mechanism, modulation of reaction rate, and physiological considerations. *J. Am. Chem. Soc.* **116**, 1414–1422.

35. Bobrowski, K., Wierzchowski, K.L., Holcman, J. & Ciurak, M. (1992) Pulse radiolysis studies of intramolecular electron transfer in model peptides and proteins. 4. Met/S-Br-$Tyr/O^{\bullet}$ radical transformation in aqueous solution of H-Tyr-$(Pro)_n$-Met-OH peptides. *Int. J. Radiat. Biol.* **62**, 507–516.

36. Stryer, L. & Haugland, R.P. (1982) Energy transfer: A spectroscopic ruler. *Proc. Natl. Acad. Sci. U.S.A.* **58**, 719–726.

37. Land, E.J. & Prütz, W.A. (1979) Reaction of azide radicals with amino acids and proteins. *Int. J. Radiat. Biol.* **36**, 75–83.

38. Butler, J., Land, E.J., Prütz, W.A. & Swallow, A.J. (1982) Charge transfer between tryptophan and tyrosine in proteins. *Biochim. Biophys. Acta* **705**, 150–162.

39. Prince, R.C. & George, G.N. (1990) Tryptophan radicals. *Trends Biochem. Sci.* **15**, 170–172.

40. Sivaraja, M., Goodin, D.B., Smith, M. & Hoffman, B.M. (1989) Identification by ENDOR of Trp191 as the free-radical state in cytochrome *c* peroxidase compound ES. *Science* **245**, 738–740.

41. Erman, J.E., Vitello, L.B., Mauro, J.M. & Kraut, J. (1989) Detection of an oxyferryl porphyrin π-cation radical intermediate in the reaction between hydrogen peroxide and a mutant yeast cytochrome *c* peroxidase. *Biochemistry* **28**, 7992–7995.

42. Debus, R.J., Barry, B.A., Sithole, I., Babcock, G.T. & McIntosh, L. (1988) Directed mutagensis indicates that the donor to P^{+}_{680} in photosystem II is tyrosine-161 of the D1 polypeptide. *Biochemistry* **27**, 9071–9074.

43. Reichard, P. (1987) Regulation of deoxyribotide synthesis. *Biochemistry* **26**, 3245–3248.

44. Karthein, R., Dietz, R., Nastainczyk, W. & Ruf, H.H. (1988) Higher oxidation states of prostaglandin H-EPR study of transient tyrosyl radical in the enzyme during the peroxydase reaction. *Eur. J. Biochem.* **171**, 313–320.

45. Nordlund, P. & Eklund, H. (1993) Structure and function of the *Escherichia coli* ribonucleotide reductase protein R2. *J. Mol. Biol.* **232**, 123–164.

46. Bobrowski, K., Holcman, J. & Wierzchowski, K.L. (1989) Temperature dependence of intramolecular electron transfer as a probe for predenaturational changes in lysozyme. *Free Radical Res. Commun.* **6**, 235–241.

47. Bobrowski, K., Holcman, J., Poznanski, J. & Wierzchowski, K.L. (1997) Pulse radiolysis studies of intramolecular electron transfer in model peptides and proteins. 7. $Trp^{\bullet}$-$TyrO^{\bullet}$ radical transformation in hen egg-white lysozyme. Effects of pH, temperature, Trp62 oxidation and inhibitor binding. *Biophys. Chem.* **63**, 153–166.

48. Poznanski, J. (1996) Conformational analysis of oligoproline-bridged peptides and its application in modeling of electron transfer between terminal amino acids (Trp,Tyr,Met), *Ph.D. Dissertation* (in Polish), Institute of Biochemistry and Biophysics, Polish Academy of Sciences, Warszawa

49. Poznanski, J., Ejchart, A., Wierzchowski, K.L. & Ciurak, M. (1993) ^{1}H- and ^{13}C-NMR investigations on *cis-trans* isomerization of proline peptide bonds and conformation of aromatic side chains in H-Trp-$(Pro)_n$-Tyr-OH peptides. *Biopolymers* **33**, 781–795.

50. Sneddon, S.F. & Brooks, C.L.III (1992) The conformations of proline-linked donor-acceptor systems. *J. Am. Chem. Soc.* **114**, 8220–8225.

51. Ramachandran, G.N. & Sasisekharan, V. (1968) Conformation of polypeptides and proteins. *Adv. Protein Chem.* **23**, 283–437.

52. Jovanovic, S.V., Steenken, S. & Simic, M.G. (1991) Kinetics and energetics of one-electron-transfer reactions involving tryptophan neutral and cation radicals. *J. Phys. Chem.* **95**, 684–687.

53. DeFelippis, M.R., Murthy, C.P., Broitman, F., Weinraub, D., Faraggi, M. & Klapper, M.H. (1991) Electrochemical properties of tyrosine phenoxy and tryptophan indolyl radicals in peptides and amino acid analogues. *J. Phys. Chem.* **95**, 3416–3419.

54. Harriman, A. (1987) Further comments on the redox potentials of tryptophan and tyrosine. *J. Phys. Chem.* **91**, 6102–6104.

55. Butler, J., Land, E.J., Prütz, W.A. & Swallow, A.J. (1986) Reversibility of charge transfer between tryptophan and tyrosine. *J.C.S. Chem. Comm.* 348–349.

56. Evenson, J.W. & Karplus, M. (1993) Effective coupling in biological electron transfer-exponential or complex distance dependence. *Science* **262**, 1247–1249.

57. Inai, Y., Sisido, M. & Imanishi, Y. (1991) Photoinduced electron transfer on a single α-helical polypeptide chain. Evidence of a through-space mechanism. *J. Phys. Chem.* **95**, 3847– 3851.

58. Lee, H., Faraggi, M. & Klapper, M.H. (1992) Long range electron transfer along an α-helix. *Biochim. Biophys. Acta* **1159**, 286–294.

59. Faraggi, M. & Klapper, M.H. (1990) Intramolecular electron transfer reactions in peptides and proteins; in *Excess Electrons in Dielectric Media* (Ferradini, C. & Jay-Cerin, J.-P., eds.) pp. 397–423, CRC Press, Boca Raton.

60. Weinstein, M., Alfassi, Z.B., DeFelippis, M.R., Klapper, M.H. & Faraggi, M. (1991) Long range electron transfer between tyrosine and tryptophan in hen egg-white lysozyme. *Biochim. Biophys. Acta* **1076**, 173–178

61. Kuroda, J., Sakiyama, F. & Narita, K. (1975) Oxidation of tryptophan in lysozyme by ozone in aqueous solution. *J. Biochem.* **78**, 641–665.

62. Sakiyama, F. & Natsuki, R. (1976) Identification of tryptophan 62 as an ozonization-sensitive residue in hen egg-white lysozyme. *J. Biochem.* **79**, 225–228.

63. Delepierre, M., Dobson, C.M., Karplus, M., Poulsen, F.M., States, D.J. & Wedin, R.E. (1987) Electrostatic effects of hydrogen exchange behaviour in proteins. The pH depenedence of exchange rates in lysozyme. *J. Mol. Biol.* **197**, 111–130

64. Wedin, R.E., Delepierre, M., Dobson, C.M. & Poulsen, F.M. (1982) Mechanisms of hydrogen exchange in proteins from nuclear magnetic resonance studies of individual trypto-

phan indole NH hydrogens in lysozyme. *Biochemistry* **21**, 1098–1103.

65. Pedersen, T.G., Thomsen, N.K., Andersen, K.V., Madsen, J.C. & Poulsen, F.M. (1993) Determination of the rate constant-k1 and constant-k2 of the Linderstrom-Lang model for protein amide hydrogen exchange — A study of the individual amides in hen egg-white lysozyme. *J. Mol. Biol.* **230**, 651–660.

66. Imoto, T., Johnson, L.N., North, A.C.T., Phillips, D.C. & Rupley, J.A. (1972) Vertebrate lysozymes; in *The Enzymes* (Boyer, P.D., ed.) pp. 665–668, Academic Press, New York

67. Banerjee, S.K., Holler, E., Hess, G.P. & Rupley, J.A. (1975) Reaction of *N*-acetylglucosamine oligosaccharides with lysozyme. *J. Biol. Chem.* **250**, 4355–4367.

68. Beratan, D.N., Betts, J.N. & Onuchic, J.N. (1991) Protein electron transfer rates set by the bridging secondary and tertiary structure. *Science* **252**, 1285–1288.

69. Betts, J.N., Beratan, D.N. & Onuchic, J.N. (1992) Mapping electron tunneling pathways. Algorithm that finds the "minimum length"/ maximum coupling pathway between electron donors and acceptors in proteins. *J. Am. Chem. Soc.* **114**, 4043–4046.

70. Beratan, D.N., Onuchic, J.N., Betts, J.N., Bowler, B.E. & Gray, H.B. (1990) Electron-tunneling pathways in ruthenated proteins. *J. Am. Chem. Soc.* **112**, 7915–7921.

71. Ramanadham, M., Sieker, L.C. & Jensen, L.H. (1990) Refinement of triclinic lysozyme: II. The method of stereochemically restrained last squares. *Acta Crystallogr. B* **46**, 63–69.

72. Daizadeh, I., Medvedev, E.S. & Stuchebrukhov, A.A. (1997) Effect of protein dynamics on biological electron transfer. *Proc. Natl. Acad. Sci. U.S.A.* **94**, 3703–3708.

73. Ichiye, T. & Karplus, M. (1983) Fluorescence depolarization of tryptophan residues in proteins: A molecular dynamics study. *Biochemistry* **22**, 2884–2893.